Macromolecules

ARTICLE

pubs.acs.org/Macromolecules

Phosphonium-Containing ABA Triblock Copolymers: Controlled Free Radical Polymerization of Phosphonium Ionic Liquids

Shijing Cheng,[†] Frederick L. Beyer,[‡] Brian D. Mather,[†] Robert B. Moore,[†] and Timothy E. Long*[,†]

[†]Department of Chemistry, Macromolecules and Interfaces Institute, Virginia Tech, Blacksburg, Virginia 24061-0344, United States

[‡]Army Research Laboratory, Materials and Manufacturing Sciences Division, Aberdeen Proving Ground, Maryland 21005-5059, United States

Supporting Information

ABSTRACT: Phosphonium ion-containing acrylate triblock (ABA) copolymers were synthesized using nitroxide mediated radical polymerization. The polymerization of styrenic phosphonium-containing ionic liquid monomers using a difunctional alkoxyamine initiator, $DEPN_2$, afforded an ABA triblock copolymer with an *n*-butyl acrylate soft center block (DP ~ 400) and symmetric phosphonium-containing external reinforcing blocks (DP < 30). Two phosphonium monomers with different alkyl substituent lengths enabled an investigation of the effects of ionic aggregation of phosphonium cations on the physical properties of ABA block copolymer ionomers. Subsequently, the thermomechanical properties and morphologies of these materials were compared to a noncharged triblock copolymer analogue with neutral polystyrene external blocks. Shortening the alkyl substituents on the phosphonium cation enhanced the hydrophilicity of tributyl-4-vinylbenzyl phosphonium chloride (BPCl) relative to trioctyl-4-vinylbenzyl phosphonium chloride (OPCl). In both cases, phosphonium cations promoted microphase-separation and thermoplastic elastomer performance for the OPCl- and BPCl-containing triblock copolymers compared to a less well-defined, microphase segregated morphology for the styrene analogue. Dynamic mechanical analysis (DMA) of phosphonium-containing triblock copolymers exhibited well-defined rubbery plateau regions, whereas the plateau was shortened for the nonionic analogue. The solid state morphologies of the block copolymers were studied using small-angle X-ray scattering (SAXS) and transmission electron microscopy (TEM), and both techniques revealed phase separation at the nanoscale. DMA studies indicated that phosphonium aggregation governed flow activation energies.

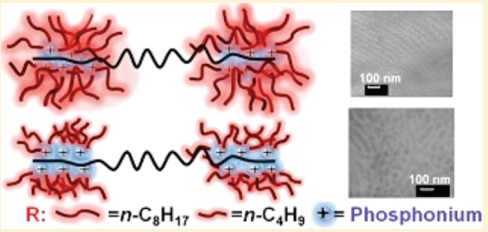

INTRODUCTION

As a result of the development of new synthetic methods for producing charged block copolymers,[1,2] there is a growing interest in microphase-separated ion-containing block copolymers as membranes for the next generation of batteries, water purification membranes, and fuel cells.[3] For these applications, ionic species are often mixed with block copolymers, such as lithium salts blended with poly(ethylene oxide)-containing copolymers;[4,5] alternatively, ionic sites are covalently attached to the block copolymer, e.g., sodium styrenesulfonate-containing block copolymers.[6−9] Because of the fact that most organic polymers are incompatible with ionic species, charged block copolymers may selectively restrict ion transport through one microphase and enable the formation of well-defined, ionic pathways for conduction.

Cation-containing polymers, which possess positively charged ammonium or phosphonium atoms, are particularly important because of their technological importance as phase-transfer catalysts,[10] antistatic agents,[11] biocides,[12] humidity sensors,[13] and water filtration membranes.[14] Polymers functionalized with amphiphilic phosphonium or ammonium units are also good candidates for alkaline fuel cell membranes.[15,16] Minteer et al. reported that the alkaline anion-exchange capacity of tetraalkylphosphonium bromide treated membranes was larger than the ammonium analogues.[15] In addition, a widely described concern with ammonium-based polymers is their chemical instability in alkaline environments, especially at elevated temperatures, which is mainly due to the reactivity of ammonium cations with hydroxide anions in a nucleophilic substitution and/or a Hofmann-type elimination. Thus, the thermal stability and chemical resistance of phosphonium salts suggest a potentially superior alternative.

By varying the alkyl groups and mobile counterions it is possible to tailor the amphiphilicity of phosphonium units for self-assembly.[17] A special class of phosphonium salts comprises low melting ionic liquids (mp < 100 °C).[18] Polymers with phosphonium units randomly distributed along the polymer main-chain are well documented. For example, McGrath et al. reported the synthesis of poly(arylene ether) main-chain phosphonium-containing ionomers for high-performance applications, such as ion-exchange membranes.[19] The phosphonium ionomers were prepared through the reduction of poly(arylene ether phosphine oxide) to phosphine/phosphine oxide copolymers with

Received: April 9, 2011
Revised: July 8, 2011
Published: July 20, 2011

phenylsilane and subsequent quaternization of phosphines with alkyl halides. In addition, quaternization of polyamides with phosphines yielded polymers bearing quaternary phosphonium cations along the polymer backbone.[20] Yan et al. recently synthesized a phosphonium-containing polysulfone that offered high alkaline conductivity, good solubility in low-boiling-point water-miscible solvents, and outstanding alkaline stability.[16] In addition, our research group recently synthesized a novel phosphonium diol as a chain extender to form polyurethane, main-chain, phosphonium ionomers, which demonstrated a facile strategy for phosphonium-containing step-growth polymers.[21]

Chain-growth polymerization represents a versatile strategy for the synthesis of phosphonium ionomers through either postpolymerization modification[22,23] or the polymerization of styrenic,[24] acrylate,[25] or methacrylate[26] phosphonium-containing monomers. Compared to the synthesis of other ionomers such as sodium styrenesulfonate, direct polymerization of phosphonium-containing monomers is attractive due to the moderate amphiphilicity of phosphonium compounds, which renders them miscible with most hydrocarbons and prevents insolubility during polymerization. Lowe et al. first demonstrated the controlled reversible addition−fragmentation chain transfer (RAFT) radical homo- and copolymerization of phosphonium-based styrenic monomers in aqueous media, and they qualitatively confirmed the pH-responsive aggregation of phosphonium-based hydrophilic diblock copolymers in aqueous solutions.[24] Yoshida et al. also found that phosphonium-containing amphiphilic diblock copolymers formed reversible spherical micelles in organic solvents.[27] Parent et al. synthesized poly(isobutylene-*co*-isoprene) phosphonium and ammonium ionomers with thermomechanical behavior comparable to vulcanized thermosets due to ionic aggregation of the phosphonium cations.[22] Matyjaszewski and co-workers reported the synthesis of phosphonium-based telechelic polystyrene and poly(methyl methacrylate) using atom transfer radical polymerization (ATRP).[23]

Our research group previously reported the noncovalent attachment of phosphonium cations to ABA block copolymers using complementary multiple hydrogen bonds.[28] These thermally reversible hydrogen bonds introduced strong temperature-dependent properties to the ionomers, which were melt processable above the hydrogen bond dissociation temperature. The present work demonstrates nitroxide mediated radical polymerization (NMP) of styrenic phosphonium ionic liquid monomers with a difunctional alkoxyamine initiator ($DEPN_2$), which results in an ABA triblock copolymer with symmetrically charged external blocks. NMP is a well-established controlled free radical polymerization methodology that facilitates block copolymer formation with a wide range of acrylic and styrenic monomers. Moreover, NMP is particularly suited for fundamental studies of ion-containing block copolymers, due to high tolerance to ionic functionalities and the absence of residual metal catalysts.[29,30] In this study, we utilized NMP and successfully synthesized a series of phosphonium-containing triblock copolymers, varying the ionic content and the lengths of the hydrophobic alkyl substituents on the phosphonium cations. We studied the influence of phosphonium cations on the thermomechanical behavior of phosphonium-containing triblock copolymers. Complementary studies of the microphase separation and structure−property relationships of the block copolymers with regards to the tunable electrostatic interactions and self-assembly of phosphonium cations were also performed using differential scanning calorimetry (DSC), dynamic mechanical analysis (DMA), transmission electron microscopy (TEM), and small-angle X-ray scattering (SAXS). The resulting materials offer promise as thermally stable thermoplastic elastomers with tunable morphology.

EXPERIMENTAL SECTION

Materials. *n*-Butyl acrylate (99%) was purchased from Aldrich and purified using an neutral alumina column and subsequent distillation at reduced pressure from calcium hydride. 4-Vinylbenzyl chloride (90%) was purchased from Aldrich and purified with an alumina column. 2,2′-Azobis(isobutyronitrile) (AIBN) (98%), 2,6-di-*tert*-butyl-4-methylphenol (99%), diethyl-*meso*-2,5-dibromoadipate (98%), copper(I) bromide (99.999%), copper powder (45 *u*m, 99%), and *N*,*N*,*N*′,*N*″,*N*″-pentamethyldiethylenetriamine (PMDETA) (98%) were purchased from Aldrich and used without further purification. Cytec Industries kindly donated trioctylphosphine (≥95%) and tributylphosphine (≥95%). The following compounds were synthesized according to previous reports: DEPN,[31] $DEPN_2$,[32] trioctyl-4-vinylbenzyl phosphonium chloride[33] (OPCl), and tributyl-4-vinylbenzyl phosphonium chloride[33] (BPCl). Hexane (Fisher Scientific, HPLC grade), tetrahydrofuran (THF) (Fisher Scientific, HPLC grade), and *N*,*N*-dimethylformamide (DMF) (Fisher Scientific, HPLC grade, anhydrous) were used as received.

Polymerization of *n*-Butyl Acrylate with $DEPN_2$. $DEPN_2$ (78 mg, 0.10 mmol) and DEPN (6 mg, 0.20 mmol) were weighed into a 100 mL, round-bottomed flask containing a magnetic stir bar. The flask was sealed with a three-way joint allowing the application of vacuum or nitrogen and the introduction of reagents using a syringe. The flask was evacuated to 60 mmHg and refilled with high-purity nitrogen three times. Purified *n*-butyl acrylate (30 mL, 210 mmol) was added and the mixture was degassed with three freeze−pump−thaw cycles. Finally, the flask was immersed in an oil bath maintained at 120 °C for 2 h. After polymerization, any residual monomer was removed at reduced pressure (60 mmHg, 40 °C, 6 h). SEC analysis in THF revealed a typical number-average molecular weight of 53 600 g/mol, M_w/M_n =1.17. Yield: 31%

Synthesis of Phosphonium-Containing Triblock Copolymers. DEPN-terminated poly(*n*-butyl acrylate) homopolymer (500 mg, M_n = 53 600 g/mol) and OPCl (900 mg, 3.6 mmol) were added to a 50 mL, round-bottomed flask with a magnetic stir bar. The flask was sealed with a three-way joint and evacuated to 60 mmHg and refilled with high-purity nitrogen three times. DMF (15 mL) was syringed into the flask, and the mixture was degassed repeatedly with freeze−pump−thaw cycles. The flask was then immersed in an oil bath at 120 °C for 2 h. After polymerization, DMF was removed upon distillation at reduced pressure. The polymer was redissolved in THF and precipitated into methanol/water mixture and finally dried at 50 °C under reduced pressure (0.5 mmHg) for 24 h. ^{1}H NMR (CD_2Cl_2) revealed block molecular weights 29.7K−53.6K−29.7K (OPCl: 21.3 mol %). BPCl-containing triblock copolymers were synthesized in a similar fashion. After polymerization, DMF was removed at reduced pressure. The polymer was redissolved in $CHCl_3$ and then precipitated into warm DI water. Yield: 56%. ^{1}H NMR (400 MHz, CD_2Cl_2, 25 °C) (δ, ppm): 0.86 (t, CH_3, 3H), 1.2−1.5 (br, COO $CH_2CH_2CH_2CH_3$, CH_2−CH−COO−, CH_2−CH−Ph−), 1.7 (br, CH_2−CH−Ph−, 1H), 2.1 (br, CH_2−CH−COO−, CH_2−CH−Ph−, 1H), 3.9 (br, $COOCH_2$, 2H), 4.7 (br, Ph−CH_2−P, 2H), 6.5 (br, Ph, 2H), 7.3 (br, Ph, 2H).

Synthesis of Phosphonium-Containing Homopolymer. OPCl or BPCl (3.7 g) was weighed into a 100 mL, round-bottomed flask containing a magnetic stir bar. The flask was sealed and purged with N_2 for 20 min. Anhydrous DMF (25 wt %) was added to the flask to dissolve the phosphonium-containing monomers. Finally, AIBN (0.58 mol %) was dissolved in 10 mL of anhydrous DMF and sparged with dry nitrogen for 10 min and added to the reaction mixture. The reaction flask was placed in an oil bath at 60 °C for 24 h with constant stirring. For OPCl homopolymerization, DMF was removed at reduced pressure after the

reaction was completed. The crude product was redissolved in THF and precipitated into a methanol−water mixture. For BPCl homopolymerization, the reaction solution was directly precipitated into THF and filtered. The final products were dried at 50 °C under reduced pressure (0.5 mmHg) for 24 h. Yield: 91% for BPCl; 73% for OPCl. ^{1}H NMR for BPCl homopolymer (400 MHz, D_2O, 25 °C) (δ, ppm): 0.86 (t, CH_3, 3H) 1.2−1.5 (br, P−CH_2−CH_2−CH_2−CH_3, 4H), 1.7 (br, CH_2−CH−Ph−, 2H), 2.1 (br, CH−Ph−, 1H), 4.7 (br, Ph−CH_2−P, 2H), 6.5 (br, Ph, 2H), 7.3 (br, Ph, 2H). %). SEC analysis in 0.05 M LiBr/DMF revealed molecular weight data M_n = 71.3K g/mol, M_w/M_n = 1.66 for BPCl homopolymer and M_w = 44.9K g/mol, M_w/M_n = 2.62 for the OPCl homopolymer.

Synthesis of Poly(styrene-*b*-*n*-butyl acrylate-*b*-styrene). DEPN-terminated poly(*n*-butyl acrylate) homopolymer (1.0 g, M_n = 53 200 g/mol), styrene (3.5 g, 33.6 mmol), and DMF (13 mL) were added to a 50 mL, round-bottomed flask with a magnetic stir bar. The flask was sealed with a three-way joint and evacuated to 60 mmHg and refilled with high-purity nitrogen three times repeatedly with freeze−pump−thaw cycles. The flask was then immersed in an oil bath at 120 °C for 2 h. After polymerization, DMF was removed with reduced pressure. The polymer was dissolved in THF and precipitated into a methanol/water mixture. ^{1}H NMR ($CDCl_3$) revealed block molecular weights 21.6K−53.2K−21.6K (styrene: 50 mol %). SEC analysis in THF revealed molecular weight data M_n = 99.1K g/mol, M_w/M_n =1.34. ^{1}H NMR (400 MHz, $CDCl_3$, 25 °C) (δ, ppm): 0.86 (t, CH_3, 3H) 1.2−1.5 (br, $CH_2CH_2CH_3$−, $CH_2CH_2CH_2$−, 2H), 1.7 (br, CH_2−CH−Ph−, 1H), 2.1 (br, CH−Ph−, 1H), 6.5 (br, Ph, 2H), 7.3 (br, Ph, 2H).

Polymer Characterization. Size exclusion chromatography (SEC) was performed in THF using a Waters size exclusion chromatograph. The instrument was equipped with an autosampler, three 5 μm PLgel Mixed-C columns, a Waters 2410 refractive index (RI) detector operating at 880 nm, a Wyatt Technologies miniDAWN multiangle laser light scattering (MALLS) detector operating at 690 nm, and a Viscotek 270 viscosity detector at 40 °C at a flow rate of 1 mL/min. The molecular weights of phosphonium-containing homopolymers was determined using SEC at 50 °C in DMF with 0.05 M lithium bromide (LiBr) at 1 mL/min. DMF SEC was performed on a Waters SEC equipped with two Waters Styragel HR5E (DMF) columns, a Waters 717plus autosampler, and a Waters 2414 differential refractive index detector. Reported molecular weights are relative to polystyrene standards. ^{1}H NMR and ^{31}P NMR spectroscopies were performed in CD_2Cl_2 on a 400 MHz Varian Inova spectrometer at 23 °C. Fast atom bombardment mass spectrometry (FAB−MS) was conducted in positive ion mode on a JEOL HX110 dual focusing mass spectrometer. Differential scanning calorimetry (DSC) was performed using a TA Instruments Q2000 differential scanning calorimeter under a nitrogen flow of 50 mL/min with a heating rate of 10 or 20 °C/min. Glass transition temperatures were measured at the midpoint of the transition in the second heat. Dynamic mechanical analysis (DMA) was conducted on a TA Instruments Q800 Dynamic Mechanical Analyzer in tension mode at a frequency of 1 Hz, an oscillatory amplitude of 15 μm, and a static force of 0.01 N. The temperature ramp was 3 °C/min. The glass-transition temperature (T_g) was determined at the peak maximum of the tan δ curve. Tensile experiments employed an Instron at 13 mm/min strain rate.

Sample Preparation and Morphological Characterization. Solution cast films of OPCl- and BPCl-containing block copolymers were prepared for SAXS and TEM study of the solid state ionomer morphology. Solutions of 5 wt % OPCl- and BPCl-containing block copolymer in $CHCl_3$ were prepared at room temperature and the solvent was allowed to evaporate slowly over a period of 2 d. The resulting films were annealed for 2 d at reduced pressure at 120 and 170 °C, respectively.

SAXS data were collected on a customized, 3 m pinhole-collimated camera. Characteristic CuK_α X-rays (λ = 1.542 Å) were generated with a Rigaku Ultrax18 rotating anode generator operated at 4.5 kW and filtered using Ni foil. A 120 mm Molecular Metrology multiwire area detector collected two-dimensional data sets for samples characterized at two sample-to-detector distances (50 and 150 cm). Camera length was calibrated using silver bihenate. The raw data were corrected for background noise and placed on an absolute scale (cm^{-1}) using a glassy carbon secondary standard. Using Wavemetrics Igor Pro software and procedures available from Argonne National Laboratory, the data were corrected and then azimuthally averaged for analysis as intensity, I, as a function of q, the magnitude of the scattering vector, where $q = 4\pi \times \sin(\theta)/\lambda$, in which 2θ was the scattering angle and λ was wavelength.[34] Finally, for each sample, the 1D data from the two camera lengths were combined into one data set spanning an angular range 0.007−0.45 $Å^{-1}$. Peak positions were determined by fitting Lorentzian distributions, along with a power-law background and a constant, to the data and minimizing error using least-squares analysis. A helium pycnometer (AccuPyc 1330 Pycnometer) was used to determine the volume and thus the density of 100 mol % BPCl and 100 mol % OPCl. This was a noninvasive procedure using purified helium as the displaced medium. After calibration, the specimens were placed in the measurement cell and purged with helium for 5−10 min. At least three experiments were conducted on each sample. The densities reported represented the averages for each sample, and standard deviations of these repeated experiments were below 2‰.

TEM specimens approximately 100 nm thick were dry sectioned from the solvent-cast and annealed films using a Reichert-Jung ultramicrotome equipped with a cryo unit operating at −75 °C. The microtomed sections were stored in a desiccator at room temperature prior to imaging. TEM experiments were performed using a Philips EM-420 scanning transmission electron microscope operated at 100 kV. Images were collected with a charge-coupled device (CCD) camera.

RESULTS AND DISCUSSION

Synthesis and Characterization of Phosphonium-Containing Triblock Copolymers. Introducing ionic functionalities to block copolymers is often challenging using postpolymerization modification or functional group protection/deprotection strategies due to limited accessibility of the functional sites.[35] In contrast, controlled radical polymerization of monomers bearing anionic, cationic, zwitterionic, and neutral functionalities is readily achieved in organic and aqueous environments under both homogeneous and heterogeneous conditions. Currently, there are only reports in the literature detailing the direct polymerization of phosphonium-containing monomers using RAFT polymerization.[24,36] In fact, to the best of our knowledge this is the first report of the synthesis of phosphonium-containing triblock copolymers using nitroxide-mediated polymerization (Scheme 1). DEPN-terminated poly(*n*-butyl acrylate) prepared with a difunctional nitroxide initiator ($DEPN_2$)[37] reinitiated phosphonium functional monomers (OPCl and BPCl) and afforded symmetrical outer blocks at each chain end. Both OPCl and BPCl monomers were soluble in most organic solvents. OPCl had a melting point of 87 °C, which classified this compound as a polymerizable phosphonium ionic liquid. In contrast, BPCl, which possesses shorter butyl substituents, had a higher melting point of 125 °C and dissolved readily in water. Copolymerization of the difunctional poly(*n*-butyl acrylate) precursor and phosphonium-containing monomers using a variety of feed ratios afforded triblock copolymers with various outer block lengths and similar center block lengths. Tables 1 and 2 summarize the monomer feed ratios, compositions, molecular weights, and glass transition temperatures. All polymerizations

Scheme 1. Synthesis of Phosphonium-Containing Triblock Copolymers and Schematic Representation of Polymer Structures

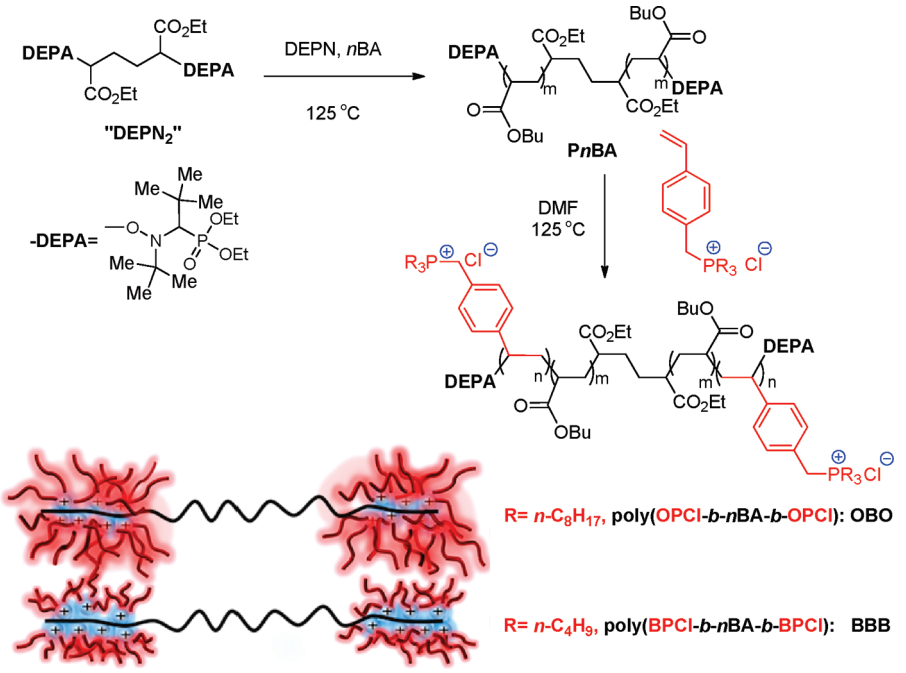

Table 1. Molecular Characterization of Poly(OPCl-*b*-*n*BA-*b*-OPCl) with Identical Molecular Weight of the Center Block (M_n= 53.6 K, M_w /M_n = 1.17)

sample name	OPCl in feed (mol %)	OPCl in polymer (mol %)	OPCl in polymer (wt %)	M_n (g/mol)	$T_{g,DSC}$ (°C)[a]	$T_{g,DMA}$ (°C)[a]
OBO-6	12	6	21	7.4K−53.6K−7.4K	−47	N/A
OBO-10	20	10	31	12.2K−53.6K−12.2K	−45	−37
OBO-21	31	21	53	29.7K−53.6K−29.7K	−43	−36
-	100	100	100	44.9K	78	N/A

[a] Only one T_g observed.

remained homogeneous in DMF. However, significant copolymer aggregation in organic solvents prevented SEC molecular weight characterization of the phosphonium-containing triblock copolymers. Thus, the block copolymer molecular weights were determined indirectly using SEC data of the central P*n*BA blocks and ^{1}H NMR spectroscopic data of the block copolymers. Comparison of the integration of ^{1}H NMR resonances at 6.0−8.0 ppm and 3.5−5.0 ppm, which corresponded to the chemical shift of four aromatic protons in one phosphonium-containing repeat unit and two protons from both *n*-butyl acrylate (−O−CH_2−) and phosphonium monomer (−phenyl−CH_2−P^+−), respectively (Figure S1, Supporting Information), revealed the ionic concentration of the triblock copolymer. ^{31}P NMR spectra of the phosphonium monomers and block copolymers revealed a single peak at 32 ppm, which corresponded to the quaternary phosphonium cation, suggesting the absence of degradation of phosphonium cations during polymerization (Figure S2, Supporting Information). The copolymerization of the OPCl and BPCl monomers was stopped at moderate conversion (50−60%) in order to control polydispersibility. All copolymers investigated were optically clear, suggesting the absence of macrophase separation.

Thermal Properties. The glass transition temperatures of the OPCl and BPCl homopolymers were 78 and 176 °C respectively (Table 1 and 2). The pendant trioctyl groups in OPCl reduced the glass transition below polystyrene; in contrast, the BPCl homopolymer bearing tributyl groups had a significantly higher glass transition temperature. DSC analysis of poly(OPCl-*b*-*n*BA-*b*-OPCl)s (OBOs) with ionic concentration varying from 6 to 21 mol % exhibited a single glass transition near −40 °C, which was associated with the glass transition of P*n*BA. The absence of a glass transition temperature associated with OPCl is not surprising in view of the relatively short OPCl-containing blocks. This independence of T_g with copolymer composition suggested that the OPCl units did not restrict segmental motion in the P*n*BA phase and that the OBOs microphase separated. Similarly, glass transition temperatures of poly(BPCl-*b*-*n*BA-*b*-BPCl) (BBB) were in the range of −50 to −45 °C. At higher ionic concentrations of 15 and 33 mol %, a second glass transition temperature appeared near 140 °C, approaching the glass transition of BPCl homopolymer at 176 °C. DSC results suggested that both the OBO and BBB samples exhibited microphase separation with a P*n*BA soft phase and an ion-rich hard phase. The presence of the second glass transition temperature, as well as the higher T_g of BPCl homopolymer compared to OPCl homopolymer, indicated that the influence of alkyl substituents on T_g was highly dependent on chain length. According to the molecular structure of OPCl and BPCl, both steric effects of bulky alkyl chains and ionic interactions influence mainchain segmental motion in the

Table 2. Molecular Characterization of Poly(BPCl-*b*-*n*BA-*b*-BPCl) with the Same Center Block (M_n= 52.7 K, M_w/M_n = 1.20)

sample name	BPCl in feed (mol %)	BPCl in polymer (mol %)	BPCl in polymer (wt %)	M_n (g/mol)	$T_{g,DSC}$ (°C)	$T_{g,DMA}$ (°C)
BBB-6	11	6	15	4.5K−52.7K−4.5K	−49	N/A
BBB-9	19	9	22	7.6K−52.7K−7.6K	−48	−25, −[a]
BBB-15	27	15	33	12.9K−52.7K−12.9K	−49, 140	−24, 49
BBB-33	65	33	58	35.9K−52.7K−35.9K	−49, 142	−26, 190
-	100	100	100	71.3K	176	N/A

[a] Broad transition.

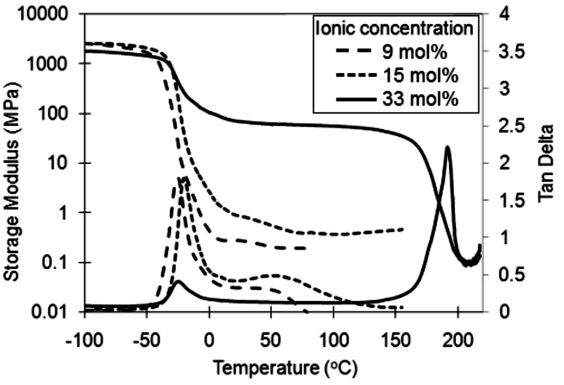

Figure 1. Dynamic mechanical temperature sweep for BBBs with 9, 15, and 33 mol % of BPCl, respectively.

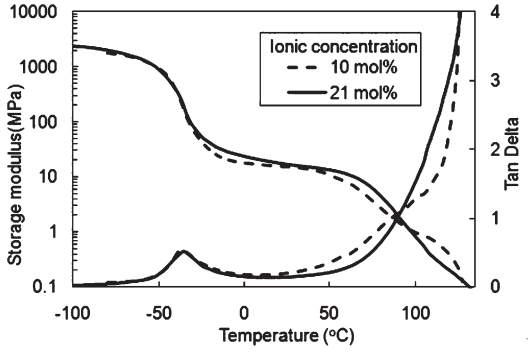

Figure 2. Dynamic mechanical temperature sweep for OBO with 10 and 21 mol % of OPCl.

hard phase. The trioctyl substituents presumably shielded the ionic aggregation of the phosphonium cations and created large free volume, which contributed to a depressed T_g. On the other hand, shorter tributyl substituents, which possessed more cationic character, enhanced the rigidity of the mainchain and presumably hindered segmental motion.

Thermomechanical Behavior. Dynamic mechanical analysis (DMA) ascertained the thermal dynamic mechanical behavior of phosphonium-containing triblock copolymers. The temperature dependencies of the storage modulus (G') and loss tangent (tan δ) for the BBBs are shown in Figure 1. The BBBs showed two distinctive tan δ peaks in all cases. The tan δ peak at −37 °C corresponded to the T_g of poly(*n*-butyl acrylate) center block, while the second relaxation peak at a higher temperature corresponded to the relaxation of the BPCl-containing hard phase. This higher temperature transition shifted from 25 to 190 °C with increasing BPCl block molecular weights, and the

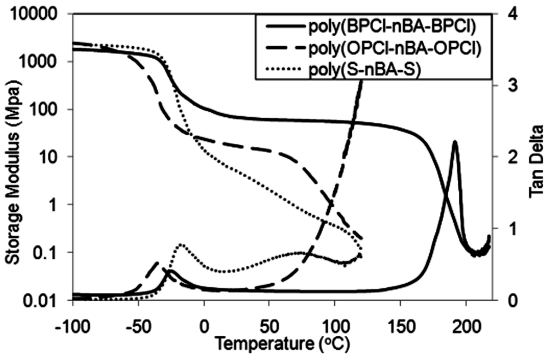

Figure 3. Dynamic mechanical temperature sweep for (1) BBB with 58 wt % of BPCl, (2) OBO with 53 wt % of OPCl, and (3) poly(S-*b*-*n*BA-*b*-S) with 50 wt % of styrene.

peak height increased with weight fraction of the BPCl block. Additionally, the plateau modulus significantly increased with hard phase weight fraction for the BBB-15 and BBB-33. The flatness of the rubbery plateau in BBB-33 also suggested more well-defined microphase separation at higher ionic concentrations, which correlated well with DSC results.

DMA data including the storage modulus and tan δ behaviors of OBOs are shown in Figure 2. The tan δ curves exhibited maxima at −37 °C, near the T_g of P*n*BA (−40 °C). A rubbery plateau was evident above T_g with an onset of flow near 100 °C. The higher temperature tan δ peaks were convoluted with polymer flow and thus were difficult to distinguish. However, the G' of the OBOs indicated that the second transition occurred at much lower temperatures in comparison to the BBBs. A similar trend was also demonstrated in ammonium neutralized sulfonated polystyrene by Weiss et al[38] and in phosphonium-containing Nafion membranes by Moore et al.,[39] i.e., relaxation temperature decreased with increasing alkyl substituent length. In addition, the G' of the OBOs spanned a 70 °C temperature window prior to viscous flow with a decrease of 12 MPa, indicating a very gradual dissociation of the hard phase. In contrast, the onset of flow for the BPCl-containing polymers resulted in a loss of storage modulus over a 20 °C temperature window with a 50 MPa decrease of G' (Figure 1). This dramatic difference in melt flow behavior points to the structural differences between the two families of block copolymers. More interestingly, when the OPCl hard phase weight fraction increased from 31 to 58 wt %, both the rubbery plateau height and length were similar. This similar plateau length indicated that the molecular weights of the outer blocks were above M_e; therefore, the second glass transition was molecular weight independent. The constant plateau modulus was attributed to relatively bulky trioctyl substituents in the hard phase that weaken the aggregation of phosphonium cations and decreased the relaxation. Additionally, tributyl substituents on

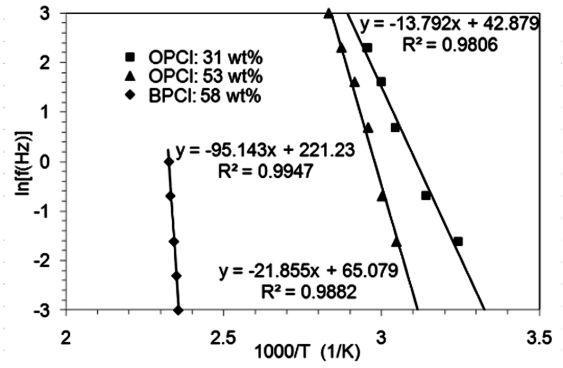

Figure 4. Influence of ionic content on flow activation energies (E_a) of phosphonium-containing triblock copolymers. E_a's are 182 ± 10 kJ/mol for 21 mol % OPCl and 115 ± 9 kJ/mol for 10 mol % OPCl and 791 ± 29 kJ/mol for 33 mol % BPCl.

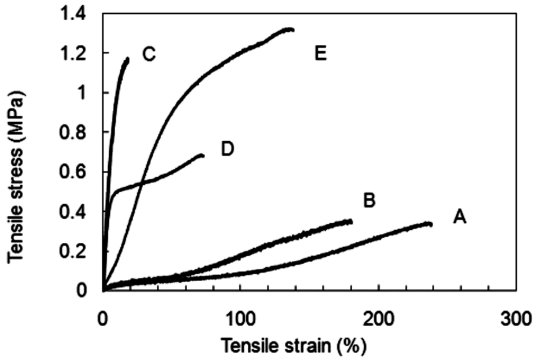

Figure 5. Engineering stress−strain curves of triblock copolymers. BBBs: (A) 9 mol %, (B) 15 mol %, and (C) 33 mol % of BPCl. OBOs: (D) 21 mol % of OPCl. Poly(S-*b*-*n*BA-*b*-S): (E) 50 mol % of styrene.

the phosphonium centers permitted more efficient physical cross-linking of the ionic sites.

In a comparative study, DMA results of the noncharged analogue (poly(S-*b*-*n*BA-*b*-S)) with a similar weight fraction of the hard phase did not show a distinct rubbery plateau; moreover, a higher glass transition temperature of the rubbery phase at −17 °C was indicative of phase mixing (Figure 3). Similar results were obtained for HCl-quaternized styrene−butadiene−2-vinylpyridine ABC block copolymers where rubbery plateau moduli increased upon quanternization.[40] McGrath et al. also found that neutralization promoted well-defined microphase separation of hydrolyzed poly(*t*BMA-*b*-BD-*b*-*t*BMA) as shown by DMA, in the absence of a morphological change.[41] DMA studies confirmed that the OBOs and BBBs displayed enhanced microphase separation compared to the neutral block copolymers. The charged block copolymers also exhibited thermoplastic elastomer behavior.

DMA at Multiple Frequencies. In order to gain greater insight into the transition from rubbery to viscous flow behavior, DMA experiments were performed over multiple frequencies varying from 0.1 to 20 Hz.[42] The transition temperature was defined as the temperature where a maximum in the loss modulus G'' occurred. Plotting the logarithm of frequency versus the inverse of transition temperature yielded a straight line in all cases, indicating Arrhenius behavior, as shown in Figure 4. The apparent activation energies (E_a's) of the higher glass transition calculated from the linear slopes were 115 ± 9 kJ/mol for OBO-10, 182 ± 10 kJ/mol for OBO-21, comparable to that of lightly sulfonated polystyrene,[43] and 791 ± 29 kJ/mol for BBB-33, respectively. We ascribed the different activation energies to structural differences in the phosphonium units since molecular weights were similar. To distinguish the influence of hydrophobic interactions from alkyl chains and ionic association from phosphonium cations, we analyzed the activation energies as a function of phosphonium charge density (Figure S10, Supporting Information). Phosphonium charge density was calculated based on the atomic concentration of phosphorus. Our results confirmed that OBO samples exhibited a linear relationship and the slope was smaller than for BBB samples, suggesting that the presence of longer alkyl chains not only diluted charge density but also hindered the association between phosphonium cations. Einsenberg et al. studied melt flow behavior in quaternized poly(4-vinylpyridinium-*b*-styrene-*b*-4-vinylpyridium) ABA triblock ionomers and observed that plasticizing ionic aggregates hindered polymer flow to a greater extent than the well-defined ionic domains.[44] In summary, dissociation of the ionic-rich phase was a thermally activated process with Arrhenius behavior, and E_a increased significantly with increasing ionic concentration and shortening *n*-alkyl chain length.

Stress−Strain Experiments. Uniaxial stress−strain experiments were performed on rectangular tensile specimens punched from cast films of phosphonium-containing triblock copolymers and their nonionic polymer analogues. Representative stress−strain curves are shown in Figure 5. The BBBs at low ionic concentrations exhibited behavior similar to covalently cross-linked rubbers with a relatively low modulus, substantial stress softening, and lack of yielding. The initial slopes of the curves increased with ionic concentration (curves A, B, and C), and the elongation at break was systematically reduced, which was attributed to the rigid BPCl domains acting as a "filler" in the rubbery acrylate matrix leading to an increased value of the modulus. The enhancement of strength at high elongations is often attributed to either strain-induced crystallization or finite extensibility of the polymer chains; the latter was assumed to have occurred for these amorphous polymers.[45] Increasing the ionic concentration resulted in significant enhancements of Young's moduli. Additionally, OBOs with 50 wt % hard phase exhibited a lower modulus and a longer strain at break compared to the corresponding BBBs (Table 3), possibly due to either shortened outer block lengths or stronger plasticization from alkyl substituents. The overall shape of the stress−strain curves of the OBOs exhibited a combination of elastomeric and yield behavior.

Morphology. Limited TEM was performed in order to obtain real-space information to complement SAXS experiments. The phosphonium cations with chloride counterions provided weak but sufficient contrast to image samples without use of a staining contrast agent. The morphology of BBB-15, shown in Figure 6a, is indeterminate but clearly microphase separated. Figure 6b shows a lamellar structure of the OBO-21. SAXS was used to investigate microphase separation and to determine, where possible, morphological organization with respect to the degree of microphase separation of the phosphonium-containing block copolymers. X-ray scattering data are shown in Figure 7, plotted as intensity, $I(q)$, versus scattering vector, q. Clear Bragg diffraction maxima were observed for the OBO-21 and BBB-15 triblock copolymers, denoting the presence of ordered morphologies. For OBO-21, the maxima were found at q^*, $2q^*$, and approximately $4q^*$, ratios typical of a lamellar morphology. The average lamellar

Table 3. Tensile Properties of Phosphonium-Containing Triblock Copolymers and Non-Ionic Analogues

sample	calculated M_n from ^{1}H NMR (g/mol) (g/mol)	hard phase (wt %)	tensile strain at break (%)	tensile stress at break (25 °C, MPa)	Young's modulus (25 °C, MPa)
BBB	7.6K−52.7K−7.6K	22	275 ± 10	0.36 ± 0.02	0.20 ± 0.05
	12.9K−52.7K−12.9K	33	186 ± 17	0.40 ± 0.11	0.30 ± 0.07
	35.9K−52.7K−35.9K	58	22.5 ± 0.8	1.10 ± 0.10	12.8 ± 0.8
OBO	29.7K−53.6K−29.7K	53	103 ± 18	0.48 ± 0.12	15.1 ± 2.0
poly(S-*b*-*n*BA-*b*-S)	21.6K−53.2K−21.6K	45	147 ± 7	0.85 ± 0.33	2.5 ± 0.4

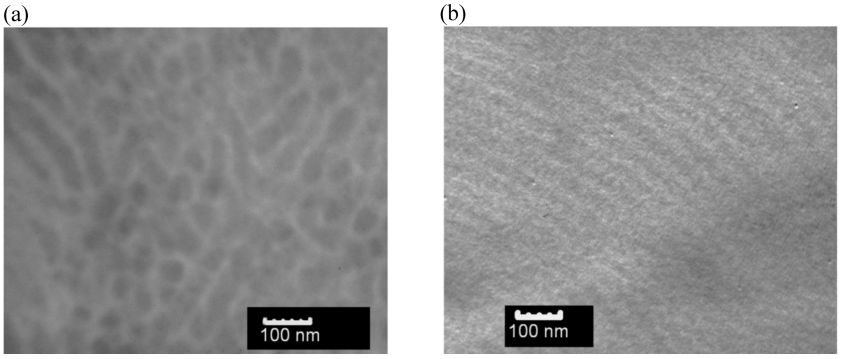

Figure 6. Transmission electron microscopy image of (a) BBB (BPCl: 15 mol %) and (b) OBO (OPCl: 21 mol %) without stain.

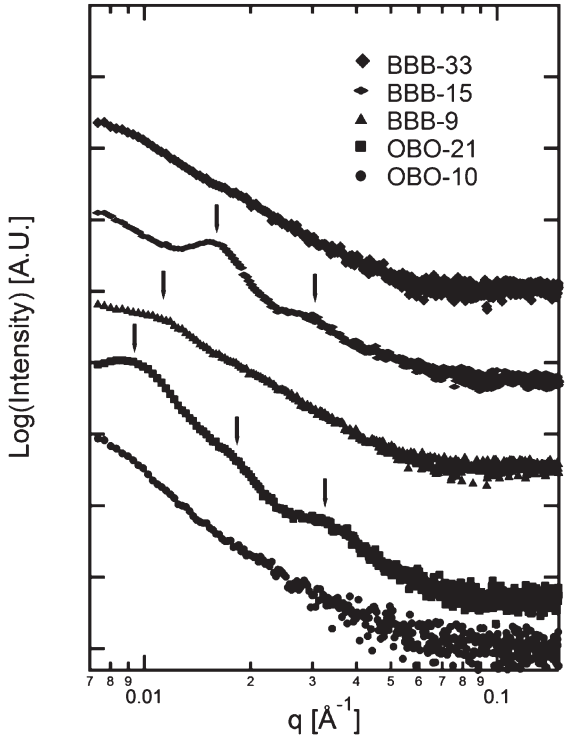

Figure 7. X-ray scattering intensity vs scattering vector (q) for (a) BBB and (b) OBO.

period, $d = 2\pi/q^*$, was calculated to be approximately 74 nm, which was larger than the expected spacing based on the volume fraction of the outerblocks, suggesting possible phase mixing or other interactions between the blocks. Sample BBB-15 exhibited maxima at q^* and roughly $2q^*$, but the number of Bragg maxima present was insufficient for the identification of an ordered morphology. A very weak feature was visible in the SAXS data for BBB-9, possibly indicating the presence of a disordered nanoscale structure.

The SAXS data provided information on microphase separation that was not wholly consistent with the physical and mechanical characterization data described above. For example, although all samples showed characteristics of microphase separation using DSC, the SAXS data for the OBO-10 and BBB-33 copolymers were featureless. BBB-33 also revealed a clear rubbery plateau in DMA behavior, indicative of the presence of physical cross-links, and a much greater elastic modulus than the lower ion-content BBB materials.

This lack of clear evidence of microphase separation in the SAXS data, especially for the BBB samples, may be a result of the X-ray scattering characteristics. X-ray scattering contrast is given by the square of the difference of the X-ray scattering length density for each phase, $(\Delta\rho)^2(\mathrm{cm}^{-4})$, where ρ is the scattering length density (cm^{-2}). Scattering length density is a function of both composition and mass density. Using density values of 1.0745 g/cm^3 for 100 mol % BPCl (measured), 1.0039 g/cm^3 for 100 mol % OPCl (measured), and 1.08 g/cm^3 for P*n*BA, the X-ray scattering contrast factor $(\Delta\rho)^2$ was calculated to be 8.95×10^{14} cm^{-4} for BPCl and *n*BA, while OPCl and *n*BA had an X-ray scattering contrast factor of 2.61×10^{19} cm^{-4}. For comparison, the X-ray scattering contrast factor for polyisoprene and PS, for which microphase separated block copolymers scatter X-rays relatively well, is 8.19×10^{19} cm^{-4}, which is more than three times that of OPCl−*n*BA and several orders of magnitude greater than that calculated for BPCl−*n*BA. In addition, the solution casting process for film formation also influences microphase separation, and this may be more significant for the bulkier side groups.

The limited TEM data combined with the SAXS data indicated generally weak microphase separation in these materials. While a

dx.doi.org/10.1021/ma200829h |*Macromolecules* 2011, 44, 6509–6517

complete determination of the thermodynamics of microphase separation for these two sets of block copolymers is beyond the scope of this manuscript; measurements of the actual functional form of χ for these two series of samples, as well as a more complete understanding of the effect of ionic interactions on morphological behavior in such materials,[46,47] would provide a clearer understanding of the morphological behaviors observed in this study.

CONCLUSIONS

Phosphonium cation-containing ABA-type triblock copolymers were synthesized for the first time using nitroxide-mediated polymerization involving a difunctional initiator and a phosphonium ionic liquid monomer. For comparative purposes, phosphonium units with tributyl and trioctyl substituents (BPCl and OPCl) were incorporated into outer blocks respectively, and poly(S-*b*-*n*BA-*b*-S), a noncharged analogue, was also synthesized. DMA analyses of phosphonium ion-containing block copolymers and the noncharged analogue showed that incorporating phosphonium units afforded microphase separated polymers with a well-defined rubbery plateau. Phosphonium ion-rich domains microphase separated from amorphous rubbery matrices and evolved to various morphologies, which was clearly shown using TEM and SAXS. The block copolymer containing 15 mol % of BPCl self-assembled into hexagonal cylindrical structures, and the copolymer bearing 21 mol % of OPCl-formed lamellae. Their corresponding SAXS peaks systematically shifted to lower q region, indicating an increase in ionic domain size with the length of alkyl substituents. Additionally, block copolymers with tributyl groups required significantly higher activation energy for flow compared to trioctyl groups. The presence of relatively more hydrophobic longer alkyl chains diluted charge density and decreased the relaxation of the ionic phase. The tensile properties of the BPCl-containing triblock copolymers confirmed their elastomeric behavior, and the OPCl-containing triblock copolymers behaved with a combination of elastomeric and yield-like behavior. The self-assembly of amphiphilic phosphonium units in block copolymer systems resulted in well-defined microphases and tuned flow behaviors, which provide potential alkaline fuel cell membrane and melt processing applications.

ASSOCIATED CONTENT

Supporting Information. Dynamic scanning calorimetry analysis, of trioctyl-4-vinylbenzyl phosphonium chloride, ^{1}H NMR spectra of OPCl, BPCl, and phosphonium-containing triblock copolymers, ^{31}P NMR spectra of phosphonium-containing triblock copolymers, glass transition temperatures, dynamic mechanical frequency sweeps, and influence of charge density on activation energies. This material is available free of charge via the Internet at http://pubs.acs.org.

AUTHOR INFORMATION

Corresponding Author

*E-mail: telong@vt.edu. Telephone: (540)231-2480. Fax: (540)231-8517.

ACKNOWLEDGMENT

The authors acknowledge the American Chemical Society Petroleum Research Fund for partial support of this research. Aspects of this work were carried out using instruments in the Nanoscale Characterization and Fabrication Laboratory, a Virginia Tech facility operated by the Institute for Critical Technology and Applied Science (ICTAS). The authors particularly thank Steve McCartney and John McIntosh at ICTAS for their help with TEM imaging. We also acknowledge funding from NSF (CHE-0722638) for the acquisition of our Agilent 6220 LC−TOF−MS. Additionally, this research was supported in part by the U.S. Army Research Laboratory and the U.S. Army Research Office under Contract/Grant Number W911NF-07-1-0452, Ionic Liquids in Electro-Active Devices Multidisciplinary University Research Initiative (ILEAD MURI).

REFERENCES

(1) Mitsukami, Y.; Donovan, M. S.; Lowe, A. B.; McCormick, C. L. *Macromolecules* **2001**, *34*, 2248–2256.
(2) Lowe, A. B.; McCormick, C. L. *Prog. Polym. Sci.* **2007**, *32*, 283–351.
(3) Elabd, Y. A.; Hickner, M. A. *Macromolecules* **2010**, *44* (1), 1–11.
(4) Singh, M.; Odusanya, O.; Wilmes, G. M.; Eitouni, H. B.; Gomez, E. D.; Patel, A. J.; Chen, V. L.; Park, M. J.; Fragouli, P.; Iatrou, H.; Hadjichristidis, N.; Cookson, D.; Balsara, N. P. *Macromolecules* **2007**, *40* (13), 4578–4585.
(5) Floudas, G.; Vazaiou, B.; Schipper, F.; Ulrich, R.; Wiesner, U.; Iatrou, H.; Hadjichristidis, N. *Macromolecules* **2001**, *34* (9), 2947–2957.
(6) Elabd, Y. A.; Napadensky, E.; Walker, C. W.; Winey, K. I. *Macromolecules* **2006**, *39* (1), 399–407.
(7) Park, M. J.; Balsara, N. P. *Macromolecules* **2008**, *41* (10), 3678–3687.
(8) Eisenberg, A.; Hird, B.; Moore, R. B. *Macromolecules* **1990**, *23* (18), 4098–4107.
(9) Saito, T.; Mather, B. D.; Costanzo, P. J.; Beyer, F. L.; Long, T. E. *Macromolecules* **2008**, *41* (10), 3503–3512.
(10) Bernard, M.; Ford, W. T.; Taylor, T. W. *Macromolecules* **1984**, *17* (9), 1812–1814.
(11) Takeuchi, K.; Shimura, S.; Kanazawa, A.; Iijima, T. JP Patent 92−358552. 1994.
(12) Kenawy, E. R.; Worley, S. D.; Broughton, R. *Biomacromolecules* **2007**, *8*, 1359–1384.
(13) Gong, M.; L., C.-W.; Joo, S.-W. *J. Mater. Sci.* **2002**, *37*, 4615–4620.
(14) Hatakeyama, E. S.; Ju, H.; Gabriel, C. J.; Lohr, J. L.; Bara, J. E.; Noble, R. D.; Freeman, B. D.; Gin, D. L. *J. Membr. Sci.* **2009**, *330*, 104–116.
(15) Moore, C. M.; Hackman, S.; Brennan, T.; Minteer, S. D. *J. Membr. Sci.* **2005**, *254*, 63–70.
(16) Gu, S.; Cai, R.; Luo, T.; Chen, Z.; Sun, M.; Liu, Y.; He, G.; Yan, Y. *Angew. Chem., Int. Ed.* **2009**, *48* (35), 6499–6502.
(17) Wathier, M.; Grinstaff, M. W. *J. Am. Chem. Soc.* **2008**, *130* (30), 9648–9649.
(18) Bradaric, C. J.; Downard, A.; Kennedy, C.; Robertson, A. J.; Zhou, Y. *Industrial Preparation of Phosphonium Ionic Liquids*. In ACS Symposium Series 856; Amercian Chemical Society: Washington, DC, 2003; pp 41−56.
(19) Ghassemi, H.; Riley, D. J.; Curtis, M.; Bonaplata, E.; McGrath, J. E. *Appl. Organomet. Chem.* **1998**, *12*, 781–785.
(20) Kenawy, E.-R.; Abdel-Hay, F. I.; Shahada, L.; El-Raheem, A.; El-Shanshoury, R.; El-Newehy, M. H. *J. Appl. Polym. Sci.* **2006**, *102* (5), 4780–4790.
(21) Williams, S. R.; Wang, W.; Winey, K. I.; Long, T. E. *Macromolecules* **2008**, *41* (23), 9072–9079.
(22) Parent, J. S.; Penciu, A.; Guillen-Castellanos, S. A.; Liskova, A.; Whitney, R. A. *Macromolecules* **2004**, *37* (20), 7477–7483.
(23) Coessens, V.; Matyjaszewski, K. *J. Macromol. Sci., Chem.* **1999**, *36* (5&6), 653–666.
(24) Wang, R.; Lowe, A. B. *J. Polym. Sci., Part A: Polym. Chem.* **2007**, *45* (12), 2468–2483.

(25) Nonaka, T.; Li, H.; Makinose, K.; Ogata, T.; Kurihara, S. *J. Appl. Polym. Sci.* **2003**, *90* (4), 1139–1147.
(26) Nonaka, T.; Li, H.; Ogata, T.; Kurihara, S. *J. Appl. Polym. Sci.* **2003**, *87* (3), 386–393.
(27) Yoshida, E.; Naito, T. *Colloid Polym. Sci.* **2008**, *286*, 1203–1207.
(28) Mather, B. D.; Baker, M. B.; Beyer, F. L.; Green, M. D.; Berg, M. A. G.; Long, T. E. *Macromolecules* **2007**, *40* (13), 4396–4398.
(29) Moad, G.; Rizzardo, E.; Thang, S. H. *Acc. Chem. Res.* **2008**, *41* (9), 1133–1142.
(30) Matyjaszewski, K.; Muller, A. H. E. *Prog. Polym. Sci.* **2006**, *31*, 1039–1040.
(31) Grimaldi, S.; Finet, J. P.; Le Moigne, F.; Zeghdaoui, A.; Tordo, P.; Benoit, D.; Fontanille, M.; Gnanou, Y. *Macromolecules* **2000**, *33*, 1141–1147.
(32) Mather, B. D.; Baker, M. B.; Beyer, F. L.; Berg, M. A. G.; Green, M. D.; Long, T. E. *Macromolecules* **2007**, *40*, 6834–6845.
(33) Kanazawa, A.; Ikeda, T.; Endo, T. *J. Polym. Sci., Part A: Polym. Chem.* **1993**, *31* (2), 335–43.
(34) Ilavsky, J.; Jemian, P. R. *J. Appl. Crystallogr.* **2009**, *42*, 347–353.
(35) Weiss, R. A.; Sen, A.; Willis, C. L.; Pottick, L. A. *Polymer* **1991**, *32* (10), 1867–1874.
(36) Stokes, K. K.; Orlicki, J. A.; Beyer, F. L. *Polym. Chem.* **2011**, *2*, 80–82.
(37) Mather, B. D.; Baker, M. B.; Beyer, F. L.; Berg, M. A. G.; Green, M. D.; Long, T. E. *Macromolecules* **2007**, *40*, 6834–6845.
(38) Weiss, R. A. *J. Appl. Polym. Sci.* **1984**, *29* (9), 2719–2734.
(39) Page, K. A.; Cable, K. M.; Moore, R. B. *Macromolecules* **2005**, *38*, 6472–6484.
(40) Gielding-Russel, G. S.; Pillai, P. S. *Polymer* **1977**, *18*, 859.
(41) Loveday, D.; Wilkes, G. L.; Deporter, C. D.; McGrath, J. E. *Macromolecules* **1995**, *28*, 7822–7830.
(42) Storey, R. F.; Baugh, D. W. *Polymer* **2001**, *42*, 2321–2330.
(43) Weiss, R. A. *Macromolecules* **1991**, *24*, 1071–1076.
(44) Gauthier, S.; Eisenberg, A. *Macromolecules* **1987**, *20*, 760–767.
(45) Noshay, A.; McGrath, J. E., *Block copolymers: overview and critical survey*; Academic Press: New York, 1977; p 516.
(46) Zhou, N. C.; Burghardt, W. R.; Winey, K. I. *Macromolecules* **2007**, *40*, 6401–6405.
(47) Tan, N. C. B.; Liu, X.; Briber, R. M.; Peiffer, D. G. *Polymer* **1995**, *36* (10), 1969–1973.